Optimal Sizing of a Parallel PHEV Powertrain

Mitra Pourabdollah, Nikolce Murgovski, Anders Grauers, and Bo Egardt, *Fellow, IEEE*

***Abstract*—This paper introduces a novel method for the simultaneous optimization of energy management and powertrain component sizing of a parallel plug-in hybrid electric vehicle (PHEV). The problem is formulated as a convex optimization problem to minimize an objective function, which is a weighted sum of operational and component costs. The operational cost includes the consumed fossil fuel and electrical energy, whereas the component cost includes the cost of the battery, electric motor (EM), and internal combustion engine (ICE). The powertrain model includes quadratic losses for the powertrain components. Moreover, the combustion engine and the electric motor losses are assumed to linearly scale with respect to the size and the losses of baseline components. The result of the optimization is the variables of the global optimal energy management for every time instant and optimal component sizes. Due to the dependency of the result on the driving cycle, a long real-life cycle with its charging times is chosen to represent a general driving pattern. The method allows the study of the effect of some performance requirements, i.e., acceleration, top speed, and all-electric range, on the component sizes and total cost.**

***Index Terms*—Convex optimization, energy management, hybrid electric vehicles, optimal control, sizing.**

I. Introduction

INTEREST in the electrification of vehicles is growing as a result of the environmental benefits that can be achieved with regard to emissions and fuel consumption. Hybrid electric vehicles (HEVs) are the first generation of electrified vehicles that have, in addition to an internal combustion engine (ICE), an electric motor (EM) and electric energy storage. HEVs can improve fuel efficiency due to the possibility of downsizing the engine, the ability to recover braking energy, the extra power control freedom gained by the two power sources, and the ability to stop the engine when idle. The next generation of electrified vehicles, i.e., plug-in hybrid electric vehicles (PHEVs), have the additional ability to store energy from the electricity grid using large-capacity batteries. The stored energy can propel the vehicle on short trips, thereby reducing vehicle dependency on petroleum and, potentially, CO_2 emissions. The extent to which this can be achieved depends on the size of the battery and the driving habits of the vehicle owner. There is clearly a tradeoff between improved fuel economy and battery cost (size). This is one of the many design tradeoffs involved with PHEVs when taking into account both cost effectiveness and performance of the vehicle [1]. These tradeoffs are highly sensitive to the varying prices of energy and components, and the driving and charging patterns. Finding the proper balance between different objectives is also related to customers' expectations. For example, if the vehicle were to be optimized for typical daily city driving, it would most likely not deliver high performance, which is rarely needed but can be attractive for many customers.[1]

The aforementioned discussion raises the following questions with regard to the design of a PHEV.

- Is component sizing mainly driven by performance requirements (PRs) such as all-electric range (AER), acceleration abilities, and top speed, or is there much freedom left to optimize the component sizes against the driving pattern?
- How much do the component costs and/or fuel consumption decrease when PRs are relaxed?
- Which PRs are cheaper to fulfill?
- What is the improvement in fuel economy when the vehicle utilizes a larger battery or EM?

The traditional approach for investigating these issues would be to consider many design candidates, each meeting a set of requirements; for example, see [3]. These candidates would then be evaluated by simulations to find the vehicle with the best overall tradeoff between cost and performance.

One aspect of (P)HEVs, which distinguishes them from conventional cars, is *energy management*, i.e., the control strategy that determines how the battery should be used (or, basically, how the power should be split between the EM and the ICE). Energy management affects both fuel economy and performance, which means that it should ideally be part of the design process in the same way as component sizing. One way of doing this is to (algorithmically) find the *optimal* energy management for each design candidate. Because real-time implementations of energy management strategies are not sought during this phase, dynamic programming (DP) is a natural candidate for finding the optimal energy management. One example of this approach is the work in [4].

One disadvantage of using DP to find the optimal energy management is that it has to be run many times during the optimization/evaluation of vehicle designs, resulting in a high computational burden. Therefore, it is a common practice to

Manuscript received April 4, 2012; revised October 15, 2012; accepted December 18, 2012. Date of publication January 30, 2013; date of current version July 10, 2013. This work was supported in part by the Swedish Energy Agency. The simulations were performed on resources provided by the Swedish National Infrastructure for Computing at the Chalmers Centre for Computational Science and Engineering. The review of this paper was coordinated by Dr. C. C. Mi.

The authors are with the Department of Signals and Systems, Chalmers University of Technology, 412 96 Gothenburg, Sweden (e-mail: mitrap@chalmers.se; nikolce.murgovski@chalmers.se; anders.grauers@chalmers.se; bo.egardt@chalmers.se).

Color versions of one or more of the figures in this paper are available online at http://ieeexplore.ieee.org.

Digital Object Identifier 10.1109/TVT.2013.2240326

[1]A survey conducted by Consumer Reports in [2] shows that half of the customers who want to buy a new car would sacrifice performance or vehicle size for better fuel economy, and 38% are even willing to pay more to get lower fuel consumption.

instead apply a suitably parameterized strategy, which is often rule based. The problem of powertrain component sizing, which relies on rule-based control, has been considered in [5]–[10]. Usually, the parameters are simultaneously optimized with the component sizes. One drawback of this method is that the choice of control structure will influence the optimal component sizes; for example, in [12], it is shown that an HEV may require a battery with larger capacity when applying a rule-based energy management strategy compared with a so-called blended strategy. Another approach is given in [13], where a rule-based energy management is first applied to find the optimal component sizes, and then, DP is used to refine the suboptimal rules for the vehicle with the obtained component sizes.

A different approach is taken in [14] to *simultaneously* optimize both battery size and energy management for a plug-in hybrid bus. The idea is to cast the problem as a convex optimization problem based on quasistatic models. Convexity has the following two important implications: 1) There is a unique optimum, and 2) fast reliable solvers are available. This, in turn, means that it is feasible to include as optimization variables not only component sizes but also the complete *control trajectory* of the energy management system. This results in a large number of variables in the problem (easily tens of thousands). Despite this case, the fast computations make it suitable to use very long driving cycles. Being able to handle long and varying driving cycles has potential benefits in giving solutions with better robustness to driving pattern variations. To remove the need for solving a mixed integer problem, the decisions on gear selection and engine on–off are made outside the convex optimization based on heuristics.

This paper is a continuation of the work in [14], extending the method to find the optimal sizes of battery, EM, and ICE for a parallel PHEV. In addition, we add different levels of PRs to the problem, and we study the effect of these constraints on component sizes and total cost. To clarify the basic ideas, an outline of the studied optimization problem is given as follows. The objective function to be minimized over a prespecified driving cycle comprises two parts. The first part reflects the cost of the key components of the vehicle, i.e., battery, EM, and ICE. This cost is the depreciation over the chosen driving cycle. The second part is the operational cost of fuel and electricity. The optimization is done over a long driving cycle, which includes opportunities for charging from the grid. The constraints are given by equations that govern the power flow in the system and the component models and by the maximum component ratings. Finally, the decision variables to be found by the optimization solver are the component sizes (battery, EM, and ICE) and the optimal energy management (torque split, battery current, braking, and charging at every time instant). Similarly, as shown in [14], the decisions for the gears and engine on–off are made based on heuristics outside the convex optimization.

The aim of this paper is to provide a tool that can be used during the initial exploratory phase of vehicle design. It allows better understanding of the effects of components and energy prices, driving patterns, and PRs on the design of a PHEV. To illustrate how the method can be used, we show how the PRs affect the component sizes.

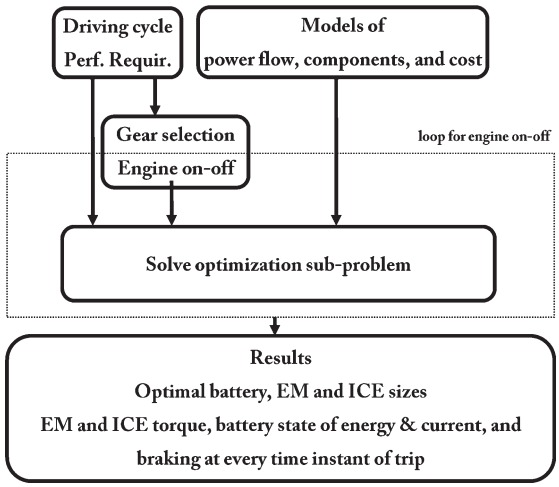

Fig. 1. Framework of the optimization problem. Gears and engine on–off are decided by heuristics, and the rest of the optimization variables are obtained by iteratively solving a subproblem.

This paper is organized as follows. In Section II, an overall view of the convex optimization problem is given. The main ingredients are described, and we discuss how, for example, the driving cycle and PRs are entered into the problem formulation. Section III continues with the convex formulation of the vehicle and component models; these models describe both the power flow and cost aspects. In Section IV, the mathematical formulation of the convex optimization problem is given in more detail. Some illustrative results from the sensitivity study are shown in Section V. Finally, conclusions are drawn.

II. Problem Statement

The optimization problem that was briefly discussed in the Introduction will now be described in some more details. We will defer the mathematical details to Section III, after having introduced the component models. As shown in Fig. 1, for a vehicle model and a given driving cycle, we first find the gears and engine on–off decisions. Having these data, in addition to the cost model and the PRs, a convex subproblem is iteratively solved to find the optimization parameters. The basic statement of the subproblem is given as follows:

$$\text{Minimize} \quad cost$$

$$\text{with respect to} \quad \begin{cases} \text{component sizes} \\ \text{energy management} \\ \text{charging from grid} \end{cases}$$

$$\text{subject to} \quad \begin{cases} \text{driving mission} \\ \text{PRs} \\ \text{selected gear and engine onoff} \\ \text{powertrain model} \\ \text{component limitations.} \end{cases}$$

Each of the ingredients of the optimization problem is described in the following sections.

TABLE I
PARAMETERS FOR CALCULATING COSTS

price of gasoline (ρ_f)	1.6 EUR/L
price of electricity (ρ_{el})	0.15 EUR/kWh
lower heating value (ρ_{LHV})	42.8×10^6 J/L
yearly interest rate (p_c)	%5
vehicle lifetime (y_v)	10 years
yearly traveled distance (s)	20 000 km

A. Optimization Cost

The optimization $cost$ to be minimized includes operational and component costs, i.e.,

$$cost = cost_{op} + cost_{comp}. \quad (1)$$

The operational cost is the sum of the fuel and electricity costs over the given driving cycle. The fuel power P_f and charger power P_g are converted to an equivalent cost in euros using energy prices ρ_f for gasoline and ρ_{el} for electricity [15]. The operational cost that is calculated over a discretized driving cycle of N sampling intervals of length $h(k)$ becomes

$$cost_{op} = \frac{\rho_f}{\rho_{LHV}} \sum_{k=1}^{N} P_f(k)h(k) + \frac{\rho_{el}}{1000 \cdot 3600} \sum_{k=1}^{N} \boldsymbol{P_g(k)} h(k) \quad (2)$$

where ρ_{LHV} is the lower heating value of gasoline. The sampling interval $h(k)$ is time varying: it is equal to 1 s while driving and to the whole parking time while charging. The detail will be given in Section III-B.

The component cost is the sum of the costs of battery, EM, and ICE; the remaining costs of the vehicle are independent of sizing and are therefore excluded from the problem. The component costs are calculated as the depreciation over the driving cycle, i.e., the proportion of the component costs given by the ratio between the length of the cycle d and the lifetime driving distance of the vehicle. Including a yearly interest rate of $p_c = 5\%$, the component cost is given by

$$cost_{comp} = \frac{d}{s y_v} \left(1 + p_c \frac{y_v + 1}{2}\right) (cost_{bat} + cost_{EM} + cost_{ICE}) \quad (3)$$

where y_v is the vehicle lifetime, and s is the average traveled distance of the vehicle in one year. For the used driving cycle of length 700 km, the depreciation is roughly 0.0045 of the total cost. The parameters in (2) and (3) are given in Table I.

B. Optimization Variables

The decision variables of the optimization problem include, first, the component sizes $\boldsymbol{s_{bat}}$, $\boldsymbol{s_{EM}}$, and $\boldsymbol{s_{ICE}}$, which are all dimensionless scaling parameters. The second group consists of optimization variables that are related to the energy management and are determined for every time instant. These variables are the torques $\boldsymbol{T_{EM}(k)}$ and $\boldsymbol{T_{ICE}(k)}$, battery current $\tilde{\boldsymbol{i}}(\boldsymbol{k})$, battery state of energy $\boldsymbol{E_b(k)}$, grid power $\boldsymbol{P_g(k)}$, and braking power $\boldsymbol{P_{brk}(k)}$. The optimization variables are marked bold in this paper.

TABLE II
VEHICLE PARAMETERS

number of days	20
number of trips	67
number of charging events (N_c)	30
distance	712.9 km
number of samples (N)	60 000 s
max. speed	120.3 kph
average speed	42.8 kph
max. acceleration	3.3 m/s^2
max. deceleration	−4.3 m/s^2

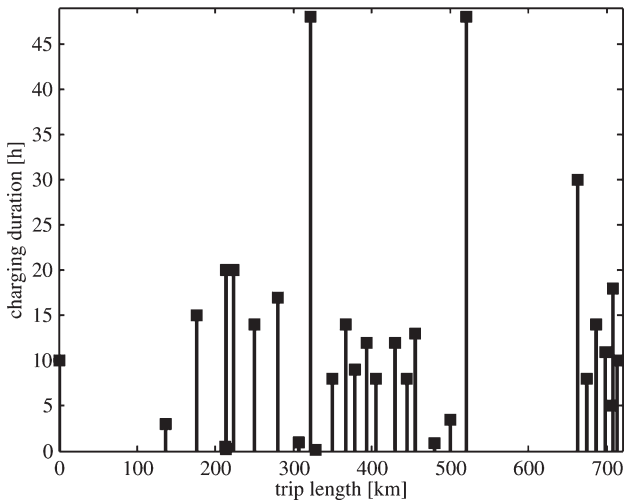

Fig. 2. Charging duration at each occasion. The vehicle can only be charged at specific locations.

C. Driving Cycle and Charging From the Grid

The optimization gives the optimal component sizes and energy management for a certain driving cycle. Ideally, the optimization should be performed over the vehicle's lifetime driving patterns. However, this is not possible due to driving uncertainties and limited computational resources. Therefore, a shorter driving cycle that includes typical driving patterns that reflect real-life driving is chosen. The driving cycle specifies the vehicle velocity $v(k)$ and, possibly, the road inclination $\beta(k)$ at discrete time instants and charging times between the trips.

The driving data used in the examples are provided by ETC[2] from a plug-in hybrid Volvo V70 and includes a long sequence of real-life driving data. We assume that the vehicle is driven on a horizontal road. The parameters of the cycle are given in Table II. At certain parking locations along the driving cycle, the vehicle has the possibility of charging from the grid. Parking durations (with charging opportunities) are taken from real data, and it is assumed that the vehicle can use the entire parking time Δt_c for charging, as shown in Fig. 2. Charging is presented in more detail in Section III-B.

D. PRs

A long driving cycle can reflect real-life driving but might not include situations that require high performance. However, high performance is still considered an important vehicle attribute by

[2]ETC Battery and FuelCells Sweden AB.

many drivers. There are basically two ways of incorporating such PRs into the optimization formulation: 1) to include explicit constraints on the component sizes and 2) to indirectly impose constraints by including some extreme driving conditions into the driving cycle. Both techniques will be used in our problem to include the following three performance parameters: 1) AER; 2) charge-sustaining top speed; and 3) acceleration at different speeds. Each of these requirements will be described in the following sections.

a) AER: The AER of a vehicle is the distance driven using only electric power from the battery. The AER is generally measured in kilometers (or miles), but it requires a reference standard driving cycle (in this paper, the New European Driving Cycle). For the vehicle studied, a battery capacity of 1 kWh corresponds to approximately 3.8-km AER. In the optimization, the required AER is translated to a lower bound on the size of the battery.

b) Top Speed: The charge-sustaining top speed v_{max} is the highest steady-state speed with the traction force provided only by the ICE. This requirement gives a lower bound on the size of the ICE.

c) Acceleration: The requirements on acceleration at different speeds (or, equivalently, requirements on constant speed at different road gradients) can be fulfilled by different combinations of ICE and EM sizes. Therefore, to include this constraint, the acceleration requirement is converted into a so-called *performance cycle*, which is appended to the real-life driving cycle. The starting point is to notice that the requirements can be represented in a single plot of *normalized net traction force* $F_{norm}(v)$ as a function of speed v. The normalized net force[3] is simply the force needed to give the vehicle the required acceleration (or ascent capability) divided by mass, i.e.,

$$F_{norm} = a + g\sin(\beta) \tag{4}$$

where a is the vehicle acceleration, g is the gravitational acceleration, and β is the road inclination. The expression in (4) shows, for example, that a powertrain that can produce a normalized net force of $F_{norm} = 1$ N/kg can accelerate with 1 m/s^2 on a flat road or maintain constant speed on a road with about 10% gradient. Therefore, specifying F_{norm} is a reasonable way of specifying powertrain performance.

The baseline requirement of F_{norm} to be used in our examples is taken from a Volvo C30 electric and is shown in Fig. 3. In this figure, we also plot different levels of PRs, obtained by multiplying the baseline curve by a coefficient α_p and changing the top speed. Finally, we also plot the accelerations from the real-life driving cycle (indicated by black dot markers) and the performance cycle (indicated by gray dot markers). The performance cycles, shown in Fig. 4, include speeds from zero to the top speed, with accelerations interpolated from the curves in Fig. 3 for different values of α_p and v_{max}. As shown in Fig. 3, the PRs are more power demanding compared to the typical driving cycles. For example, out of 60 000 acceleration points of the real-life driving cycle, at only 13 points, the demanded acceleration is higher than the 70% of the baseline acceleration

[3]The total traction force also includes friction and air resistance effects.

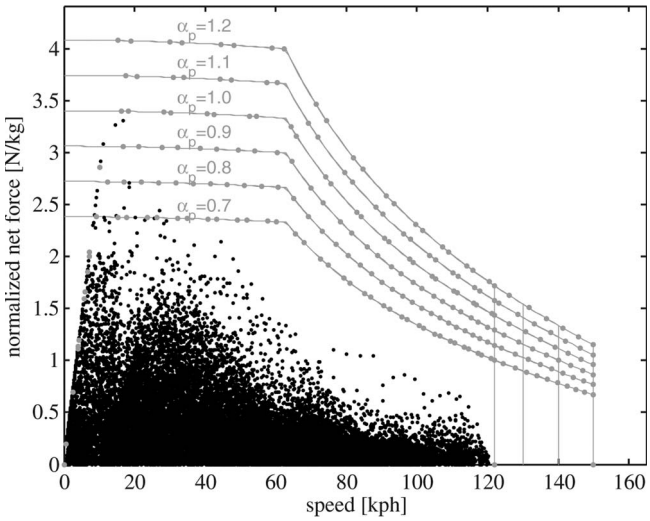

Fig. 3. Acceleration requirements (solid curves), acceleration of different performance driving cycles (gray dots), and acceleration of the real-life driving cycle (black dots) versus speed.

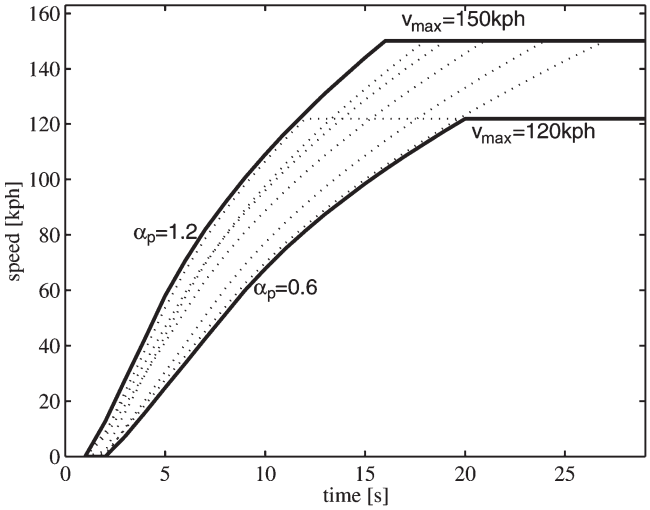

Fig. 4. Performance cycles constructed from the acceleration and top-speed requirements used for forcing the optimization to fulfill the requirements.

requirement ($\alpha_p = 0.7$). For an acceleration requirement with $\alpha_p = 0.8$ and $\alpha_p = 0.9$, the numbers are 4 and 3, respectively. If, at any time instant in the simulations, the acceleration is higher than the one from the requirements, we lower it by time stretching. The effect of this action on the results is very small, because the number of affected points is low.

E. Gear Selection

In general, gear-shifting strategies that are functions of unknown optimization variables such as torque or efficiency may lead to a nonconvex problem. The alternative is to decide the gear $\gamma(k)$ outside the convex optimization from a speed-dependent hysteresis model applied on the known driving profile [18]. However, this strategy highly influences the optimal size of the ICE, because it does not consider the engine peak power. Therefore, we modify it so that the gear strategy also depends on power; as a result, gear shifting happens at higher

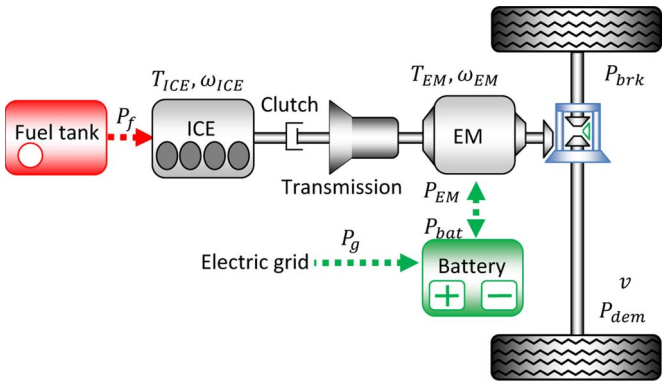

Fig. 5. Parallel PHEV configuration (solid lines refer to mechanical link, and dashed lines refer to electrical links).

speeds for high acceleration demands. The detail of this strategy is provided in the Appendix.

F. Powertrain Constraints and Components Limitations

The constraints in the optimization problem also include the equations that govern the power flow in the system, the component models, limitations of the components (e.g., current and torque), and constraints on the component sizes. These will be explained in detail in the following section.

III. Modeling Details

Modeling of the powertrain and its components is a crucial step of the presented method, because convexity has to be guaranteed. This section presents the powertrain model, the gear-shifting strategy, and the component models. Particular attention is given to a novel method to describe the power losses of EM and fuel power of ICE with convex functions,[4] including the scaling of size. In Section III-E, the cost and mass models of these components are also presented.

A. Powertrain Model

As depicted in Fig. 5, the studied PHEV includes a powertrain with parallel topology, where both the ICE and EM are mechanically linked to the drive train and can propel the wheels. From the drive cycle, velocity $v(k)$, acceleration $a(k)$, and road slope $\beta(k)$ are obtained at discrete time instants k. The required traction force $F_t(k)$ can then be calculated as [17]

$$F_t(k) = \frac{c_d A_f \rho v(k)^2}{2} + m_{tot} g c_r \cos(\beta(k)) + m_{tot} g \sin(\beta(k)) + m_{tot} a(k) \quad (5)$$

where m_{tot}, A_f, c_d, ρ, g, and c_r are the total vehicle mass, frontal area, air drag coefficient, air density, gravitational acceleration, and rolling resistance coefficient, respectively (details on the computation of m_{tot} are given in Section III-E). It follows that the powertrain has to supply the demanded power $P_{dem}(k) = F_t(k)v(k)$, which is subject to the following mechanical and electrical power balance equations of the powertrain:

$$P_{dem}(k) + \boldsymbol{P_{brk}}(\boldsymbol{k}) = \boldsymbol{T_{EM}}(\boldsymbol{k})\omega_{EM}(k) + e_{on}(k)\boldsymbol{T_{ICE}}(\boldsymbol{k})\omega_{ICE}(k)\eta(k) \quad (6)$$

$$\omega_{EM}(k)\boldsymbol{T_{EM}}(\boldsymbol{k}) + P_{EM,loss}(k) + P_{aux}(k) = P_{bat}(k) + \boldsymbol{P_g}(\boldsymbol{k})\eta_g \quad (7)$$

where $\boldsymbol{P_{brk}}(\boldsymbol{k})$ is the power dissipated at the friction brakes; $\boldsymbol{T_{EM}}(\boldsymbol{k})$, $\omega_{EM}(k)$, and $P_{EM,loss}(k)$ are the torque, speed, and power losses of the EM, respectively; $\boldsymbol{T_{ICE}}(k)$ and $\omega_{ICE}(k)$ are the torque and speed of the ICE; $P_{aux}(k)$ is the electrical power used by auxiliary devices ($P_{aux}(k)$ is assumed to be equal to 500 W when driving); $P_{bat}(k)$ is the battery power; $\boldsymbol{P_g}(\boldsymbol{k})$ is the grid power (including the losses), which is nonzero only at charging times; and η_g is the charger efficiency, which is assumed to be constant for simplicity. It is also assumed that the EM and auxiliaries are turned off during charging. The decision variable $e_{on}(k)$ is used to turn the ICE on or off, and $\eta(k)$ is the transmission efficiency, which depends on the choice of gear. For simplicity, the losses in the power electronics are included in the EM losses, and the rotational inertia (summation of the inertia of the wheels, the differential, the EM, and the ICE) are neglected in the models. The vehicle parameters are given in Table III.

TABLE III
Parameters of the Cycle

parameter	value
baseline mass (m)	1600 kg
glider mass (m_g)	1280 kg
frontal area (A_f)	2.37 m^2
rolling resistance (c_r)	0.009
aerodynamic drag coefficient (c_d)	0.33
air density (ρ)	1.293 kg/m^3
wheel radius (r_w)	0.3 m
ratio of the final gear (r_{fg})	4.2
EM reduction gear (r_{EM})	2

At each time instant of the driving cycle, the gear $\gamma(k)$ is selected based on the vehicle speed and demanded power of the powertrain with the baseline components. Details are given in the next section. Knowing the gear and the vehicle speed, the angular speeds $\omega_{EM}(k)$ and $\omega_{ICE}(k)$ can be calculated as

$$\omega_{EM}(k) = r_{EM}\frac{r_{fg}}{r_w}v(k) \quad (8)$$

$$\omega_{ICE}(k) = r_\gamma(\gamma(k))\frac{r_{fg}}{r_w}v(k) \quad (9)$$

where r_w, r_{fg}, r_{EM}, and $r_\gamma(\gamma(k))$ are the wheel radius, ratio of the final gear (differential), EM reduction gear, and ratio of the transmission gear, respectively [17]. The model does not allow any slip in the clutch; therefore, the vehicle is propelled by the EM at low speeds (typically when starting from standstill).

[4] A convex function satisfies $f(\lambda x + (1-\lambda)y) \leq \lambda f(x) + (1-\lambda)f(y)$ for all $x, y \in \mathbf{R}$ with $0 \leq \lambda \leq 1$ (see [6]).

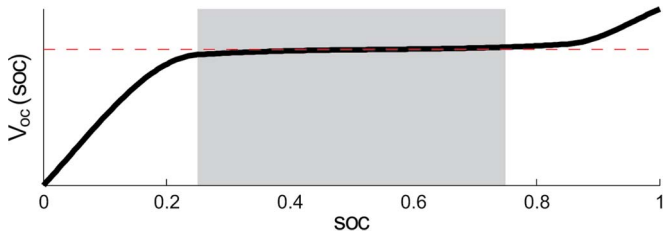

Fig. 6. Model of the battery open-circuit voltage. The original model and the approximation are represented by a solid line and a dashed line, respectively. The gray area shows the allowed SoC operating region.

B. Battery

The battery consists of $\boldsymbol{s_{bat}} = n_s \cdot n_p$ identical cells, where n_s is the number of cells in a string connected in series, and n_p is the number of strings connected in parallel. Considering the battery cell model as an open circuit voltage V_{oc} in series with a constant internal resistance R [17], the terminal power P_{bat} and the stored energy of the battery E_b can be calculated as

$$P_{bat}(k) = \boldsymbol{s_{bat}}\left(V_{oc} i(k) - R i^2(k)\right) = V_{oc}\tilde{\boldsymbol{i}}(\boldsymbol{k}) - R\frac{\tilde{\boldsymbol{i}}^{\boldsymbol{2}}(\boldsymbol{k})}{\boldsymbol{s_{bat}}} \tag{10}$$

$$\boldsymbol{E_b}(\boldsymbol{k}+\boldsymbol{1}) = \boldsymbol{E_b}(\boldsymbol{k}) - h(k) V_{oc}\tilde{\boldsymbol{I}}(\boldsymbol{k}). \tag{11}$$

The cell current $i(k) \in [i_{min}, i_{max}]$ is chosen to be positive when discharging. The current $\tilde{\boldsymbol{i}}(\boldsymbol{k}) = \boldsymbol{s_{bat}} i(k)$ is a variable change that is introduced to replace the nonconvex product of two variables $(\boldsymbol{s_{bat}} i(k))$ by a quadratic-over-linear function $(\tilde{\boldsymbol{i}}^{\boldsymbol{2}}(\boldsymbol{k})/\boldsymbol{s_{bat}})$, which is convex in both $\tilde{\boldsymbol{i}}(\boldsymbol{k})$ and $\boldsymbol{s_{bat}}$. It is clear that the battery model does not depend on the configuration of the cells (series/parallel) but, rather, on the total number of cells. The voltage over each cell V_{oc} is, in practice, a function of the state of charge (SoC) of the battery; however, in this paper, it is approximated to be constant. This assumption can be justified when operating in limited SoC ranges, as illustrated in Fig. 6.

During the available parking periods $\Delta t_c(k)$, it is assumed, without loss of generality, that the vehicle is charged with constant current and power. Then, to save computation time by not simulating over the many charging samples during a charging period, it is assumed that the whole charging energy enters the battery in one extra long sample $\Delta t_c(k)$ at the parking events. This way, at charging occasions in (11), $h(k)$ is equal to $\Delta t_c(k)$.

C. EM

The EM model with its power electronics is described by a power loss map $P_{EM,loss,base}$, where the losses are measured at steady state for different torque–speed combinations. The power losses for each EM speed can be approximated by a second-order polynomial in the torque as

$$P_{EM,loss,base}(\omega_{EM}, T_{EM,base}) = c_1(\omega_{EM}) T^2_{EM,base} + c_2(\omega_{EM}) T_{EM,base} + c_3(\omega_{EM}) \tag{12}$$

where the coefficients $c_1 \geq 0$, c_2, and c_3 are functions of ω_{EM} and, therefore, are time dependent $(c(k))$. The accuracy of this approximation is high and is discussed in [14]. The coefficients are calculated using a least squares method for grids over ω_{EM} to fit the polynomial in (12) to the measured data. For speed values that do not belong to the grid nodes, the coefficients are obtained by linear interpolation.

To vary the size of the EM, the maximum and the minimum torque $T_{EM,max,base}(\omega_{EM}(k))$ and $T_{EM,min,base}(\omega_{EM}(k))$ are scaled by a scaling factor $\boldsymbol{s_{EM}}$ [11]. The losses are assumed to linearly change with $\boldsymbol{s_{EM}}$ [21]. Hence, given a baseline EM described by torque $T_{em,base}$ and losses $P_{EM,loss,base}$, the losses of the scaled EM are calculated at each time instant as

$$\begin{aligned} P_{EM,loss}(k) &= \boldsymbol{s_{EM}} P_{EM,loss,base}(k) \\ &= \boldsymbol{s_{EM}}\left(c_1(k) T^2_{EM,base}(k) + c_2(k) T_{EM,base}(k) + c_3(k)\right) \\ &= \boldsymbol{s_{EM}}\left(c_1(k)\left(\frac{\boldsymbol{T_{EM}}(\boldsymbol{k})}{\boldsymbol{s_{EM}}}\right)^2 + c_2(k)\frac{\boldsymbol{T_{EM}}(\boldsymbol{k})}{\boldsymbol{s_{EM}}} + c_3(k)\right) \\ &= c_1(k)\frac{\boldsymbol{T^2_{EM}}(\boldsymbol{k})}{\boldsymbol{s_{EM}}} + c_2(k)\boldsymbol{T_{EM}}(\boldsymbol{k}) + c_3(k)\boldsymbol{s_{EM}}. \end{aligned} \tag{13}$$

This nonlinear model is convex in $\boldsymbol{T_{EM}}$ and $\boldsymbol{s_{EM}}$ for $\boldsymbol{s_{EM}} > 0$.

D. ICE

The fuel power P_f of an ICE is a function of the engine torque and the engine speed and is derived from a map that is obtained from engine experiments at the steady state. The fuel power represented by Willans lines [19], [20] can be approximated for each engine speed with a second-order polynomial in T_{ICE} as

$$P_{f,base}(\omega_{ICE}, T_{ICE,base}) = b_1(\omega_{ICE}) T^2_{ICE,base} + b_2(\omega_{ICE}) T_{ICE,base} + b_3(\omega_{ICE}) \tag{14}$$

where the coefficients $b_1 \geq 0$, b_2, and b_3 are functions of ω_{ICE}, are, hence, time dependent $(b(k))$, and are calculated in a similar way as c_1, c_2, and c_3 for the EM. The accuracy of this approximation is also discussed in [14].

To vary the ICE size, linear torque scaling is used [13], [21], which means that the torque is given by

$$\boldsymbol{T_{ICE}}\left(\boldsymbol{\omega_{ICE}}(\boldsymbol{k})\right) = \boldsymbol{s_{ICE}} T_{ICE,base}\left(\omega_{ICE}(k)\right) \tag{15}$$

where $\boldsymbol{s_{ICE}}$ is the scaling factor. This approach is more accurate if the size is not very far from the baseline size and for an ICE with a fixed number of cylinders; therefore, we limit the range of the $\boldsymbol{s_{ICE}}$. One alternative solution would be to update the engine map using engine simulators such as Turbocharged Diesel Engine Simulation [22], [23] and solve the optimization again in case the optimal engine size is not close

to the nominal value. Using linear scaling, the losses linearly scale, i.e., the efficiency of the ICE η_{ICE} is

$$\eta_{ICE}(\omega_{ICE}, \boldsymbol{T_{ICE}}) = \eta_{ICE,base}\left(\omega_{ICE}, \frac{\boldsymbol{T_{ICE}}}{\boldsymbol{s_{ICE}}}\right). \quad (16)$$

This way, using (14), the fuel power is calculated as

$$\begin{aligned} P_f(k) =& \frac{\omega_{ICE}(k)\boldsymbol{T_{ICE}}(\boldsymbol{k})}{\eta_{ICE}(\omega_{ICE}, \boldsymbol{T_{ICE}})} \\ =& \frac{\omega_{ICE}(k)\boldsymbol{s_{ICE}}T_{ICE,base}}{\eta_{ICE,base}\left(\omega_{ICE}, \frac{\boldsymbol{T_{ICE}}}{\boldsymbol{s_{ICE}}}\right)} \\ =& \boldsymbol{s_{ICE}}P_{f,base}(k) \\ =& \boldsymbol{s_{ICE}}\left(b_1(k)T^2_{ICE,base}(k)\right. \\ & \left. + b_2(k)T_{ICE,base}(k) + e_{on}(k)b_3(k)\right) \\ =& \boldsymbol{s_{ICE}}\left(b_1(k)\left(\frac{\boldsymbol{T_{ICE}}(\boldsymbol{k})}{\boldsymbol{s_{ICE}}}\right)^2\right. \\ & \left. + b_2(k)\frac{\boldsymbol{T_{ICE}}(\boldsymbol{k})}{\boldsymbol{s_{ICE}}} + e_{on}(k)b_3(k)\right) \\ =& b_1(k)\frac{\boldsymbol{T^2_{ICE}}(\boldsymbol{k})}{\boldsymbol{s_{ICE}}} + b_2(k)\boldsymbol{T_{ICE}}(\boldsymbol{k}) + e_{on}(k)b_3(k)\boldsymbol{s_{ICE}}. \end{aligned} \quad (17)$$

The reason for introducing the variable e_{on} is to remove the idling losses b_3 when the ICE is off. The decision for turning the ICE on, $e_{on}(k) = 1$, or off, $e_{on}(k) = 0$, has to be made prior to the optimization to preserve the problem convexity, and it is decided based on the baseline power demand required by the vehicle when following the driving cycle $P_{dem,base}(k)$. The baseline mass m that is used to calculate $P_{dem,base}(k)$ is the mass of the vehicle with the baseline component sizes, and it is given in Table III. At every time instant, if the power demand is higher than a power threshold P_{on}, the ICE is turned on; otherwise, it is turned off. This is shown as

$$e_{on}(k) = \begin{cases} 1, & \text{if } P_{dem,base}(k) > P_{on} \\ 0, & \text{otherwise.} \end{cases} \quad (18)$$

A good value of P_{on} can be chosen such that the engine is on 95% of the times (see [24]). We can also iterate the optimization over several values of P_{on} to find the best result.

E. Cost and Mass Model

Finally, we need to define how the costs and masses of the battery, EM, and ICE depend on the scaling parameters. Linear cost and weight models are used by many authors, e.g., in [25] and [26], and give accurate estimates, as long as the optimal sizes are of the same order of magnitude as the baseline (50%–200%), i.e.,

$$\begin{aligned} cost_j &= cost_{j,i} + cost_{j,s}, s_j \\ m_j &= m_{j,s}, \boldsymbol{s_j} \end{aligned} \quad (19)$$

TABLE IV
PARAMETERS OF THE COST AND MASS MODEL

$cost_{bat-i}$	€500	$m_{bat,s}$	0.687 kg
$cost_{bat-s}$	€63.7		
$cost_{EM-i}$	€1750	$m_{EM,s}$	48 kg
$cost_{EM-s}$	€875		
$cost_{ICE-i}$	€575	$m_{ICE,s}$	97.5 kg
$cost_{ICE-s}$	€666.7		

where $j \in \{bat, EM, ICE\}$, and the values for $cost_{j,i}$, $cost_{j,s}$, and $m_{j,s}$ are given in Table IV. The total mass of the vehicle m_{tot} is therefore calculated as

$$m_{tot} = m_g + m_{bat} + m_{EM} + m_{ICE} \quad (20)$$

where m_g is the glider mass (the vehicle minus its drivetrain) given in Table III. The cost and mass functions are calculated from a baseline EM of 35-kW power, and a baseline ICE with a displacement size equal to (SI) 1.6 L, and power equal to 65 kW. The battery is energy optimized with a cell capacity of $Q = 159$ Wh. Note that the choice of the battery type will influence the result of the optimization (see [27] and [28]).

IV. CONVEX OPTIMIZATION PROBLEM

In this section, the problem that was formulated in Section II is presented in more detail. The optimization problem is convex, which, in its general form, can be written as

$$\begin{aligned} \inf_x \quad & f_0(x) \\ \text{subject to} \quad & f_i(x) \le 0, i = 1, \ldots, m \\ & h_j(x) = 0, j = 1, \ldots, p \end{aligned} \quad (21)$$

where the cost function $f_0(x)$ and the constraints $f_1, \ldots, f_m : R^n \to R$ are convex, and $h_1, \ldots, h_n$ are affine functions. The cost to be minimized in the optimization problem includes the operational and component costs for a vehicle driven on a cycle. The decision variables x to be found by the optimization solver are $\boldsymbol{s_{bat}}, \boldsymbol{s_{ICE}}, \boldsymbol{s_{EM}}$, which are scalars, and $\boldsymbol{T^N_{ICE}}, \boldsymbol{T^N_{EM}}, \tilde{\boldsymbol{i}}^{\boldsymbol{N}}$, $\boldsymbol{P^N_{brk}}$, $\boldsymbol{E^{N+1}_b}$, and $\boldsymbol{P^{N_c}_g}$, which are vectors. The superscripts show the length of the vectors, where N is the number of time samples of the driving cycle. In our problem, there are slightly more than 300 000 variables, which are found by the solver in one round of optimization in about 25 min.[5]

As aforementioned, the constraints $f_1, \ldots, f_m$ and $h_1, \ldots, h_n$ in (21) include the equations that govern the power flow in the system, i.e., (6) and (7), the component models, i.e., (10), (11), (13), (17), and (19), and the limitations of the components. Recall that, for a convex problem in (21), nonlinear functions must not be tied with equalities. Clearly using (10) and (13) in (7) yields a nonlinear equality constraint. Therefore, the equality is relaxed to an inequality as

$$\omega_{EM}(k)\boldsymbol{T_{EM}}(\boldsymbol{k}) + P_{EM,loss}(k) \le P_{bat}(k) - P_{aux}. \quad (22)$$

[5]On a standard personal computer with 4-GB random access memory and 2.66 GHz.

TABLE V
CONVEX PROBLEM FOR THE PARALLEL PHEV

Variables	$\boldsymbol{T_{ICE}^N}$, $\boldsymbol{T_{EM}^N}$, $\boldsymbol{P_{brk}^N}$, $\tilde{\boldsymbol{i}}^{\boldsymbol{N}}$, $\boldsymbol{E_b^{N+1}}$, $\boldsymbol{P_g^{N_c}}$, $\boldsymbol{s_{bat}}$, $\boldsymbol{s_{ICE}}$, $\boldsymbol{s_{EM}}$
minimize	$cost(.)$
subject to	$P_{dem}(k) - \boldsymbol{P_{brk}(k)} = \boldsymbol{T_{EM}(k)}\omega_{EM}(k) + e_{on}(k)\boldsymbol{T_{ICE}(k)}\omega_{ICE}(k)\eta(k)$
	$\omega_{EM}(k)\boldsymbol{T_{EM}(k)} + P_{EM,loss}(k) + P_{aux}(k) \leq P_{bat}(k) + \boldsymbol{P_g(k)}\eta_g$
	$P_{EM,loss}(\boldsymbol{T_{EM}(k)}, \boldsymbol{s_{EM}}) = c_1(k)\frac{T_{EM}^2(k)}{s_{EM}} + c_2(k)\boldsymbol{T_{EM}(k)} + c_3(k)\boldsymbol{s_{EM}}$
	$P_{bat}(\boldsymbol{i(k)}, \boldsymbol{s_{bat}}) = V_{oc}\tilde{\boldsymbol{i}}(\boldsymbol{k}) - R\frac{\tilde{i}^2(k)}{s_{bat}}$
	$\boldsymbol{E_b(2:k+1)} = \boldsymbol{E_b(1:k)} - h(k)\tilde{\boldsymbol{i}}\boldsymbol{(1:k)}V_{oc}$
	$\boldsymbol{T_{EM}(k)} \in [T_{EM,min,base}(\omega_{EM}(k)), T_{EM,max,base}(\omega_{EM}(k))]\boldsymbol{s_{EM}}$
	$\boldsymbol{T_{ICE}(k)} \in [0, \boldsymbol{s_{ICE}}T_{ICE,max,base}(\omega_{ICE}(k))]$
	$\tilde{\boldsymbol{i}}(\boldsymbol{k}) \in [i_{min}, i_{max}]\boldsymbol{s_{bat}}$
	$\boldsymbol{E_b(k)} \in [SoC_{min}, SoC_{max}]V_{oc}Q$
	$\boldsymbol{P_g(k)} \in [0, P_{g,max}(k)]$
	$\boldsymbol{s_{bat}} \in [s_{bat,min}, s_{bat,max}]$
	$\boldsymbol{s_{EM}} \in [s_{EM,min}, s_{EM,max}]$
	$\boldsymbol{s_{ICE}} \in [s_{ICE,min}, s_{ICE,max}]$
	$\forall k \in \{0, \ldots, N-1\}$

TABLE VI
OPTIMAL COSTS AND COMPONENT SIZES FOR THE SRIVING CYCLE, WITH AND WITHOUT CONSIDERING THE PRS

variables	with PR	without PR
battery capacity	5.3 kWh	6.4 kWh
EM power	32.5 kW	32.5 kW
ICE power	128.1 kW	61.6 kW
fuel cost	€ 22.1	€ 17.4
electricity cost	€ 5.8	€ 6.1
component costs	€ 32.3	€ 31.0
total cost	€ 60.2	€ 54.7

It is easy to see that, at the optimum, the constraint will be satisfied with equality, because otherwise, the battery will unnecessarily throw away energy.

Moreover, to keep the problem convex, $\boldsymbol{s_{bat}}$ is relaxed to a real value. The relaxation will introduce a rounding error that has a small influence on the optimal result. This is because either the cell capacity can be considered very small to give a large number of cells or the result can be interpreted as an indication of the optimal pack capacity. The convex problem, as shown in Table V, is automatically translated by a tool CVX [29] to a form required by a publicly available solver Sedumi [30].

V. NUMERICAL RESULTS

In this section, we give results of the simultaneous optimization of energy management and component sizing over the aforementioned driving cycle. Different PRs are considered, either as constraints on the component sizes or through an appended performance cycle, as described in Section II.

1) PRs*:* In Table VI, the results of the optimization for the real-life driving cycle, with and without considering the baseline PRs ($\alpha_p = 1$, $v_{max} = 120$ km/h, and no AER requirements) are shown. The values in the table show that the PRs have a high influence on the size of the components and the costs. The main difference is in the size of the ICE. This is mainly because the battery cells are energy optimized with very limited power, and during the performance cycle, because the power demand is high, the number of battery cells must be large. On the other hand, a heavy and large capacity battery is not needed in the rest of the driving cycle. Therefore,

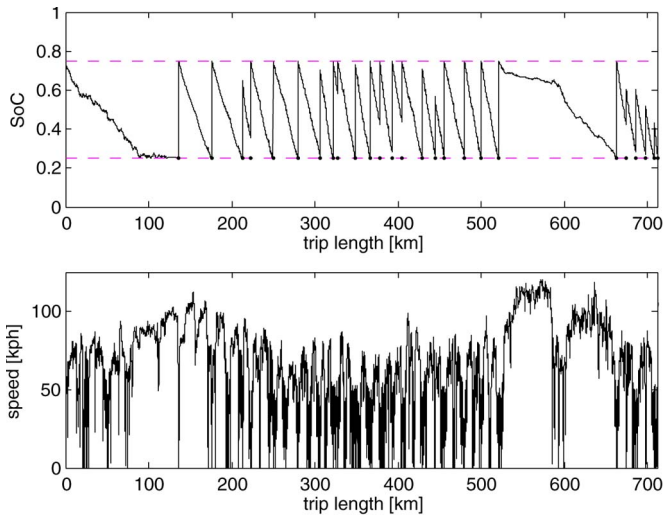

Fig. 7. Optimal SoC trajectory. The battery has the possibility of being charged from the grid at positions shown by dot (upper plot) and demanded speed profile (lower plot).

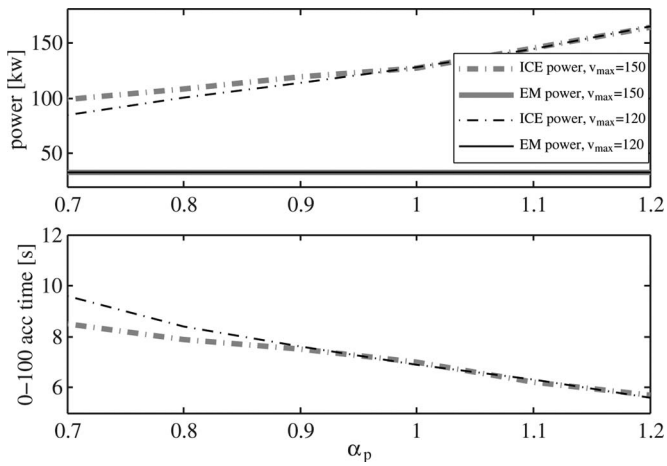

Fig. 8. Power of the ICE and EM for top speeds of 120 km/h (thin line) and 150 km/h (thick line) versus α_p (upper plot) and 0–100 km/h acceleration time versus α_p (lower plot).

the optimization finds it cheaper to provide the power for the performance cycle by the ICE. Due to a larger ICE and smaller battery capacity, the fuel consumption increases, and the electricity usage decreases. In Fig. 7, the driving cycle (without the performance cycle) and the optimal SoC trajectory are shown.

To see the effect of different levels of PRs, the optimization is done over driving cycles, including performance cycles with $\alpha_p = [0.7, 0.8, 0.9, 1.0, 1.1, 1.2]$ and top speed of $v_{max} = 120$ and 150 km/h. The result of the optimization is shown in Figs. 8 and 9. In Fig. 8, the power of the EM and the ICE and the 0–100 km/h acceleration time are plotted versus α_p. For high values of α_p, the power of the ICE noticeably increases, whereas the power of the EM does not change. Again, this is because of the type of battery. On the other hand, the top speed demand only affects the ICE size for small values of α_p, and for larger values of α_p, the ICE is sized by the acceleration requirements, and it does not change for different top-speed requirements. Clearly, increasing the acceleration demand

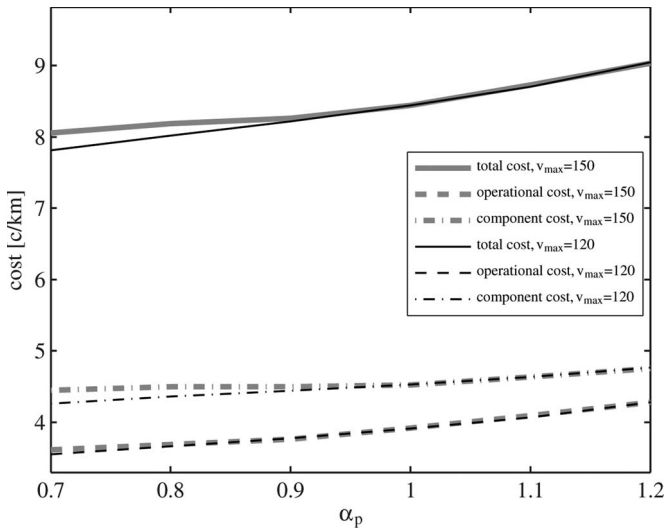

Fig. 9. Total cost, component costs, and operational cost versus α_p for top speeds of 120 km/h (thin line) and 150 km/h (thick line).

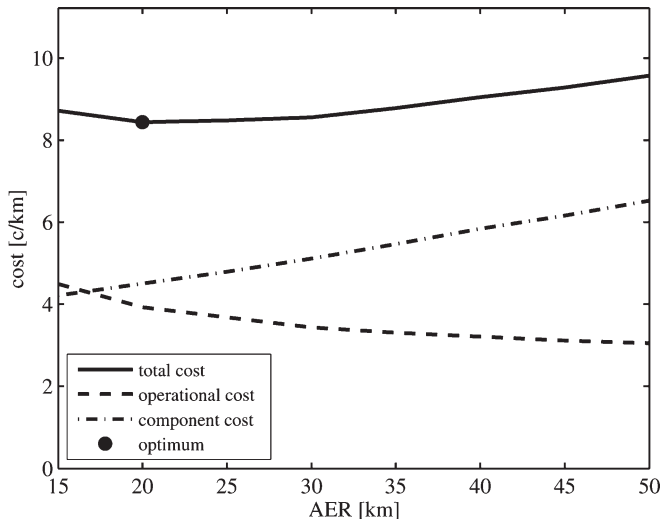

Fig. 10. Components, operational, and total optimal costs (in euro cents per kilometer) versus the AER. The minimum cost is shown with a circle.

decreases the resulting 0–100 km/h acceleration time. This plot is an indication of the performance of the vehicle. Fig. 9 shows that higher acceleration and top-speed requirements increase both the components and operational costs. The increase in the operational cost is because larger ICEs have more working points at lower efficiency (compared to smaller ICEs) and, hence, higher fuel consumption. In the figures, costs are given in euro cents per kilometer for easier comparison.

Another requirement on PHEVs is the AER, which is directly related to the size of the battery. To see the effect of this requirement, the optimization is done with different fixed battery sizes. For all the cases, the acceleration and top-speed requirements are kept constant as $v_{max} = 120$ km/h and $\alpha_p = 1$. The results in Fig. 10 show that increasing the battery capacity decreases the operational cost; on the other hand, the component costs linearly increase. The total cost decreases until it reaches the optimal battery size, here 5.2 kWh, which is equivalent to approximately 20 km of the AER. For larger battery sizes, the

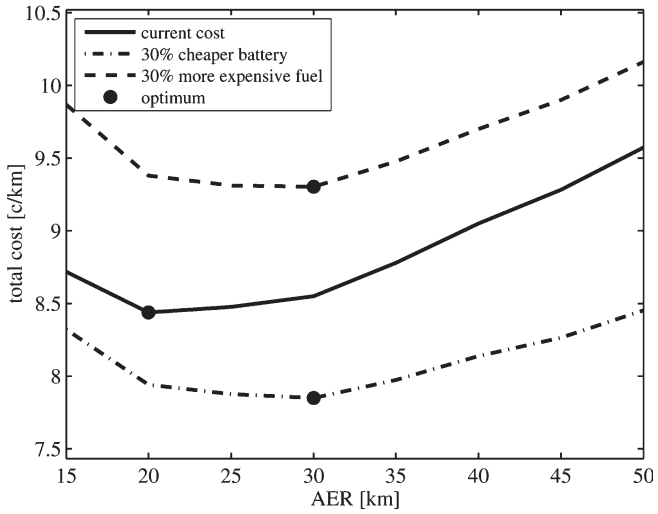

Fig. 11. Total cost with the present battery and fuel cost, 30% cheaper batteries, and 30% more expensive fuel. The minimum costs are shown with circles.

increase in the components cost is more than the gain in the operational cost, and for very large batteries, the operational cost starts increasing due to the increase in the battery mass. However, the curve is rather flat between 15- and 35-km AER, which is because low AER leads to low vehicle cost but higher operational cost, and *vice versa*. This means that, in this range of AER, the cost is not very sensitive to the requirement on AER.

2) Battery and Fuel Price: To study the effect of change in battery and fuel price, the optimization is done for three different cases. In the first case, the prices of the electricity and battery are the present prices, i.e., $\rho_f = 1.34$ EUR/L and $cost_{bat} = 400$ EUR/kWh. In the second case, the optimization includes 30% cheaper battery price, and in the third case, the optimization includes 30% more expensive fuel price. As shown in Fig. 11, in the last two cases, the optimal AER is around 30 km, which means that it is optimal to have a large AER for higher fuel cost or cheaper battery price. It can also be observed that, with the current price, a vehicle with 50-km AER costs 14% more than the optimal design, whereas for the other two cases, the difference is only 5%.

3) Pareto Front: The value of the weighting factor w_{comp} in (3) is defined for a fixed lifetime and yearly driving length. However, in real life, this value is different for different vehicles. By varying w_{comp}, a Pareto front is obtained for the optimal operational cost versus the optimal component costs; this is shown in Fig. 12 for different acceleration requirements. The figure shows that component and operational costs are conflicting objectives, as expected. In other words, components that are more expensive can lower the operational cost. The component costs increases mainly due to the increase in the battery and EM size, which clearly reduces fuel consumption. Based on (3), we can see that, for a vehicle with a longer lifetime driving distance, the value of w_{comp} is smaller, and therefore, it is optimal to pay more for the components and get a lower operational cost compared with a vehicle with a shorter lifetime driving distance. Naturally, higher PRs increase both the component and operational costs.

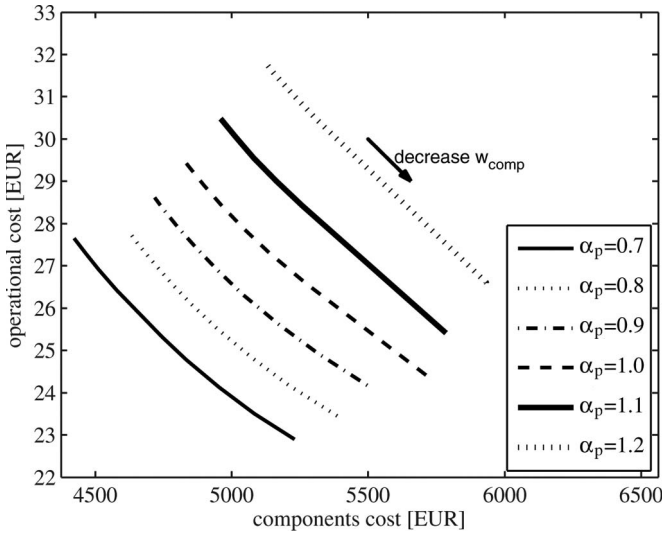

Fig. 12. Set of Pareto points using different weighting factors between the operational and component costs.

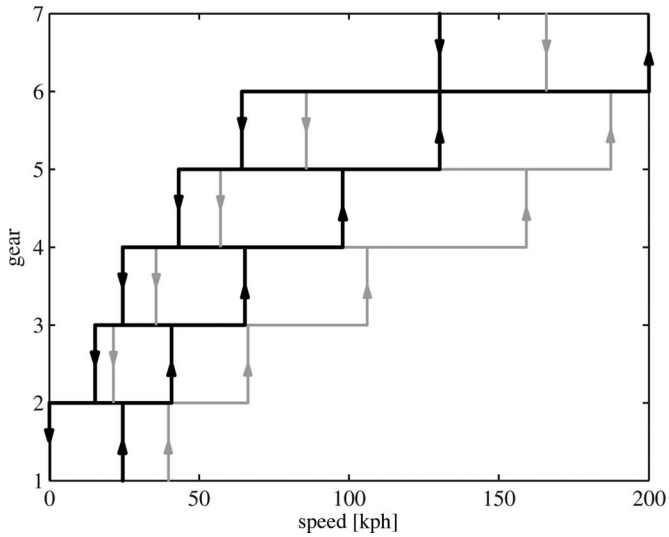

Fig. 13. Speed- and power-dependent gear-shifting strategy.

VI. Conclusion

In this paper, a new method of simultaneous optimization of component sizes (for battery, EM, and ICE) and energy management (torque split and charging) for a parallel PHEV has been introduced. The gear and engine on–off are found by heuristics, and the remaining subproblem is formulated as a convex optimization problem by approximating the quasistatic models with nonlinear convex functions. The convex formulation allows fast solutions of large-size problems, giving short turnaround design cycles. The method also has the advantage of handling very long driving cycles, which is necessary to find optimal component sizes that are robust to the varying real-life driving cycles.

The result of the optimization depends on many factors, e.g., PRs, charging behavior, driving cycle, battery type, energy and component costs, and gear shifting. The method is used to study the effect of these factors on the design of a PHEV. In particular, the effect of the PRs on the sizing of vehicle components is studied. For the examples shown in this paper, the results indicate that the vehicle cost is more affected by the acceleration requirements than the requirements on top speed and AER. This means that PRs have to be included in the optimization problem; otherwise, the result will be misleading. Moreover, with the current price of energy and battery cells, it is not optimal to have very long AER for PHEVs.

In general, the method can be used as a tool to give a better understanding of the influence of different factors on vehicle design. In addition, our current work addresses the limitation that is posed by the need to fix the gears and engine on–off prior to optimization.

Appendix
Gear Selection Strategy

As aforementioned, the gear $\gamma(k)$ is selected from a speed-dependent hysteresis model [18], as shown in Fig. 13. In this strategy, each time the speed exceeds an upper limit $v_{gu}(\gamma)$, there will be an upshift in the gear, and if the speed is lower than a lower limit $v_{gl}(\gamma)$, there will be a downshift. Knowing the gear ratios, these limits (here called base limits and shown with black lines) are chosen so that the speed of the engine is kept in normal operating regions. For example, $v_{gu}(\gamma)$ is a result of a gear strategy where there is an upshift each time the engine speed exceeds 4000 r/min, shown as a vertical line ω^b_{gu} in Fig. 14. However, this strategy highly influences the size of the ICE, because it motivates higher torques. Fig. 14 shows that, for a given power demand, if the gear is shifted up in higher speeds, the torque demand will be lower. To lessen this effect, we increase the engine speed threshold at which an upshift occurs, linearly with respect to an acceleration gain, $a_{gain} = (a(k)/a_{(\alpha_p=1)}(v(k)))$, for $a_{gain} > 0.7$. This means that, for high acceleration demands, the gear shifting happens at higher engine speeds. As shown in Fig. 13, the limits linearly

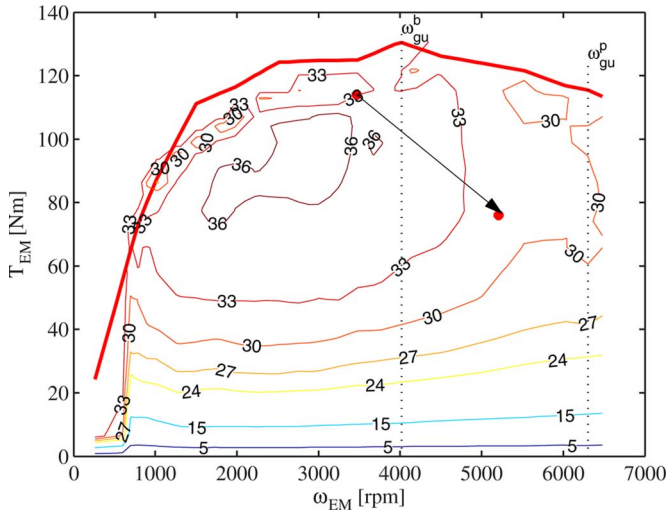

Fig. 14. Baseline limit for changing the gear in low acceleration demand ω^b_{gu}. For a similar power demand, we get a lower torque if we change the gear at higher speed ω^p_{gu}. The two situations are shown by red markers.

change between the base limits v^b_{gu} and v^b_{gl} (black lines) and peak limits v^p_{gu} and v^p_{gl} (gray lines) as

$$v_{gu}(\gamma) = \begin{cases} v^b_{gu}, & \text{if } a_{gain}(k) < 0.7 \\ \frac{v^p_{gu}(\gamma) - v^b_{gu}(\gamma)}{1.2-0.7} \\ \times (a_{gain}(k) - 0.7) + v^b_{gu}(\gamma), & \text{else} \end{cases} \tag{23}$$

$$v_{gl}(\gamma) = \begin{cases} v^b_{gl}, & \text{if } a_{gain}(k) < 0.7 \\ \frac{v^p_{gl}(\gamma) - v^b_{gl}(\gamma)}{1.2-0.7} \\ \times (a_{gain}(k) - 0.7) + v^b_{gl}(\gamma), & \text{else.} \end{cases} \tag{24}$$

Optimal gear shifting is not considered in this paper, because it may lead to a nonconvex problem. Possibilities of improving the gear-shifting strategy by first defining a feasible gear, then iteratively solving a convex problem, and using the result to update the gear selection will be considered in future studies.

ACKNOWLEDGMENT

The authors would like to thank Dr. L. Johannesson for the fruitful discussions and the reviewers for their many suggestions to improve the readability of this paper.

REFERENCES

[1] T. C. Moore, "Tools and strategies for hybrid electric drive system optimization," Soc. Automotive Eng., Warrendale, PA, USA, SAE Tech. Paper 961660, 1996.
[2] P. Valdes-Dapena, We Want Better Mileage—But Power and Size, Too, May 2007. [Online]. Available: http://www.CNNMoney.com
[3] T. Miller, G. Rizzoni, and Q. Li, "Simulation-based hybrid electric vehicle design search," Soc. Automotive Eng., Warrendale, PA, USA, SAE Tech. Paper 1999-01-1150, 1999.
[4] O. Sundström, L. Guzzella, and P. Soltic, "Torque-assist hybrid electric powertrain sizing: From optimal control toward optimal sizing law," *IEEE Trans. Control Syst. Technol.*, vol. 18, no. 4, pp. 837–849, Jul. 2010.
[5] L. Wu, Y. Wang, X. Yuan, and Z. Chen, "Multiobjective optimization of HEV fuel economy and emissions using the self-adaptive differential evolution algorithm," *IEEE Trans. Veh. Technol.*, vol. 60, no. 6, pp. 2458–2470, Jul. 2011.
[6] X. Hu, Z. Wang, and L. Liao, "Multiobjective optimization of HEV fuel economy and emissions using evolutionary computation," Soc. Automotive Eng., Warrendale, PA, USA, SAE Tech. Paper 2004-01-1153, 2004.
[7] V. Galdi, L. Ippolito, A. Piccolo, and A. Vaccaro, "A genetic-based methodology for hybrid electric vehicles sizing," *Soft Comput.*, vol. 5, no. 6, pp. 451–457, 2009.
[8] M. Montazeri-Gh and A. Poursamad, "Application of genetic algorithm for simultaneous optimization of HEV component sizing and control strategy," *Int. J. Alternative Propulsion*, vol. 1, no. 1, pp. 63–78, 2006.
[9] J. Hellgren and B. Jacobson, "A systematic way of choosing driveline configuration and sizing components in hybrid vehicles," Soc. Automotive Eng., Warrendale, PA, USA, SAE Tech. Paper 2000-01-3098, 2000.
[10] R. Fellini, N. Michelena, P. Papalambros, and M. Sasena, "Optimal design of automotive hybrid powertrain systems," in *Proc. 1st Int. Symp. Environ. Conscious Design Inverse Manuf.*, Los Alamitos, CA, USA, Feb. 1–3, 1999, pp. 400–405.
[11] C. S. N. Shiau, N. Kaushal, C. T. Hendrickson, S. B. Peterson, J. F. Whitacre, and J. J. Michalek, "Optimal plug-in hybrid electric vehicle design and allocation for minimum life cycle cost, petroleum consumption, and greenhouse gas emissions," *J. Mech. Design*, vol. 132, no. 9, pp. 091013-1–091013-11, Sep. 2010.
[12] S. J. Mouraa, D. S. Callawayb, H. K. Fathya, and J. L. Steina, "Tradeoffs between battery energy capacity and stochastic optimal power management in plug-in hybrid electric vehicles," *J. Power Sources*, vol. 195, no. 9, pp. 2979–2988, Nov. 2009.
[13] Z. S. Filipi, L. S. Louca, B. Daran, C. C. Lin, U. Yildir, B. Wu, M. Kokkolaras, D. N. Assanis, H. Peng, P. Y. Papalambros, and J. L. Stein, "Combined optimization of design and power management of the hydraulic hybrid propulsion system for a 6 × 6 medium truck," *Int. J. Heavy Veh. Syst.*, vol. 11, no. 3/4, pp. 372–402, 2004.
[14] N. Murgovski, L. Johannesson, J. Sjöberg, and B. Egardt, "Component sizing of a plug-in hybrid electric powertrain via convex optimization," *Mechatronics*, vol. 22, no. 1, pp. 106–120, Feb. 2012.
[15] Europe's Energy Portal. [Online]. Available: http://www.energy.eu/
[16] S. Boyd and L. Vandenberghe, *Convex Optimization*. Cambridge, U.K.: Cambridge Univ. Press, 2009.
[17] L. Guzzella and A. Sciarretta, *Vehicle Propulsion Systems*. Berlin, Germany: Springer-Verlag, 2007.
[18] O. Sundström, L. Guzzella, and P. Soltic, "Optimal hybridization in two parallel hybrid electric vehicles using dynamic programming," in *Proc. 17th World Congr., Int. Federat. Automat. Control*, Seoul, Korea, Jul. 6–11, 2008, pp. 4642–4647.
[19] J. B. Heywood, *Internal Combustion Engine Fundamentals*. New York, NY, USA: McGraw-Hill, 1988.
[20] S. J. Pachernegg, "A closer look at the Willans-Line," Soc. Automotive Eng. Techn. Paper 690182, 1969. DOI:10.4271/690182.
[21] O. Sundström, "Optimal control and design of hybrid electric vehicles," Ph.D. dissertation, ETH Univ., Zurich, Switzerland, 2009.
[22] D. Assanis and J. Heywood, "Development and use of a computer simulation of the turbocompounded diesel system for engine performance and component heat transfer studies," Soc. Automotive Eng., Warrendale, PA, USA, SAE Techn. Paper 860329, 1986.
[23] D. Assanis, G. Delagrammatikas, R. Fellini, Z. Filipi, J. Liedtke, N. Michelena, P. Papalambros, D. Reyes, D. Rosenbaum, A. Sales, and M. Sasena, "An optimization approach to hybrid electric propulsion system design," *Mech. Struct. Mach.*, vol. 27, no. 4, pp. 393–421, 1999.
[24] D. Karbowski, C. Haliburton, and A. Rousseau, "Impact of component size on plug-in hybrid vehicles energy consumption using global optimization," in *Proc. 23rd Int. Elect. Veh. Symp.*, Anaheim, CA, USA, Dec. 2007.
[25] P. Albertus, J. Couts, V. Srinivasan, and J. Newman, "Component sizing optimization of plug-in hybrid electric vehicles," *J. Appl. Energy*, vol. 88, no. 3, pp. 799–804, Mar. 2011.
[26] S. E. Plotkin and M. K. Singh, "Multipath transportation futures study: Vehicle characterization and scenario analyses," Argonne Nat. Lab., Lemont, IL, USA, Rep. ANL/ESD/09-5, Dec. 3, 2009.
[27] E. Tara, S. Shahidinejad, S. Filizadeh, and E. Bibeau, "Battery storage sizing in a retrofitted plug-in hybrid electric vehicle," *IEEE Trans. Veh. Technol.*, vol. 59, no. 6, pp. 2786–2794, Jul. 2010.
[28] P. Albertus, J. Couts, V. Srinivasan, and J. Newman, "A combined model for determining capacity usage and battery size for hybrid and plug-in hybrid electric vehicles," *J. Power Sources*, vol. 183, no. 2, pp. 771–782, Sep. 2008.
[29] M. Grant and S. Boyd, CVX: Matlab software for disciplined convex programming, version 1.21, CVX Res. [Online]. Available: http://cvxr.com/cvx
[30] I. Polik, Sedumi, Joomla!, Jun. 2010. [Online]. Avaialble: http://sedumi.ie.lehigh.edu/

Mitra Pourabdollah received the B.Sc. degree in electrical engineering from Shiraz University, Shiraz, Iran, in 2006 and the M.Sc. degree in systems, control, and robotics from the Royal Institute of Technology, Stockholm, Sweden, in 2009. She is currently working toward the Ph.D. degree with the Department of Signals and Systems, Chalmers University of Technology, Gothenburg, Sweden.

Her research interests include control and optimization of hybrid electric powertrains.

Nikolce Murgovski received the M.Sc. degree in applied physics from Chalmers University of Technology, Gothenburg, Sweden, the M.Sc. degree software engineering from University West, Trollhättan, Sweden, in 2007, and the Ph.D. degree in signals and systems from Chalmers University of Technology in 2012.

He currently holds a postdoctoral position with the Department of Signals and Systems, Chalmers University of Technology. His research interests include control and optimization, particularly automotive powertrains.

Anders Grauers received the M.Sc. degree in electrical engineering and the Ph.D. degree in electrical machines and drives from Chalmers University of Technology, Gothenburg, Sweden, in 1990 and 1996, respectively.

From 2002 to 2009, he was with the Volvo Car Corporation, Gothenburg, Sweden, where he worked with system development and as a Technical Specialist. He was responsible for the system design of the first generation of radar-based active safety systems, particularly the development of adaptive cruise control. Since 2009, he has been with the Swedish Hybrid Vehicle Centre, where he is focussing on system-oriented research on electric and hybrid powertrains. He is currently an Associate Professor of hybrid and electric vehicle systems with the Department of Signals and Systems, Chalmers University of Technology. His research interests include driving forces for development, system requirements, different technical solutions, and optimization of complete powertrains.

Bo Egardt (SM'90–F'03) received the M.Sc. degree in electrical engineering and the Ph.D. degree in automatic control from Lund Institute of Technology, Lund, Sweden, in 1974 and 1979, respectively.

During 1980, he was a Research Associate with the Information Systems Laboratory, Stanford, CA, USA. From 1981 to 1989, he was with Asea Brown Boveri, where he was heavily involved in the introduction of adaptive control in the process industry. In 1989, he was a Professor of automatic control with Chalmers University of Technology, Gothenburg, Sweden. He has been an Associate Editor for the *European Journal of Control*. He is a Member of the Editorial Board for the *International Journal of Adaptive Control and Signal Processing*. His research interests include adaptive and hybrid control and applications of control in the automotive area.

Dr. Egardt has been an Associate Editor for the IEEE TRANSACTIONS ON CONTROL SYSTEMS TECHNOLOGY.